Dynamics of Atactic Polystyrene in Solution

Giuseppe Allegra,*† Julia S. Higgins,‡ Fabio Ganazzoli,† Emilio Lucchelli,† and Sergio Brückner†

Dipartimento di Chimica del Politecnico, 20133 Milano, Italy, and Department of Chemical Engineering and Chemical Technology, Imperial College, London SW7 2BY, United Kingdom. *Received June 27, 1983*

ABSTRACT: The solution dynamics of atactic polystyrene ($5 \times 10^4 \leq M_w \leq 10^5$) is investigated by comparing theoretical calculation with quasi-elastic neutron scattering results in the intermediate range ($0.05 < Q$ [$=4\pi \sin(\vartheta/2)/\lambda$] < 0.3 Å^{-1}). The good-solvent expansion, the hydrodynamic interaction short of the Zimm limit, and the internal viscosity are taken into consideration; the intramolecular elasticity of an $-[A-B]_N-$ stereochemically irregular chain is also taken into account for all the configurational modes in terms of the generalized characteristic ratio. It is shown that for $Q > 0.1$ Å^{-1} the hydrodynamic interaction is quickly vanishing while the intramolecular elasticity and the internal viscosity are by far the dominating factors. Their joint effect induces an increasing chain rigidity with increasing Q, leading to a value of $\mathcal{B}$ as small as 2 for the approximate power law $t_{1/2}Q^{\mathcal{B}} = \text{const}$, where $t_{1/2}$ is the half-peak time of the dynamic coherent structure factor.

Introduction

When investigated over short distances and/or short observation times, linear macromolecules tend to depart from a universal behavior.[1] While investigation of this behavior is more complex than at a large scale, it may offer a chance of understanding some specific conformational features of the polymer in question. In the framework of a systematic investigation of polymer dynamics, both experimentally[2-5] and theoretically,[6-10] in the present study we shall discuss some recent quasi-elastic neutron scattering results obtained by one of us (J.S.H.) from dissolved atactic polystyrene chains within the reciprocal vector range $0.05 < Q$ [$=4\pi \sin(\vartheta/2)/\lambda$] < 0.3 Å^{-1}. As previously suggested, in this region the chain should depart appreciably from the bead-and-spring model although its interatomic correlation functions are still reasonably well described within a generalized Gaussian approximation.[7,8] It is worth pointing out that (i) the commonly adopted linear form of the dynamic equations is rigorously compatible only with a Gaussian interatomic probability distribution, (ii) even though the accuracy of such a distribution at equilibrium may be poor if the two atoms are contiguous along the chain sequence, it is important to stress that it steadily improves with time in the time-dependent case, because the Brownian forces impart random impulses to the chain atoms,[8] and (iii) in the present context the Gaussian approximation has a quite different meaning from that currently attributed to the bead-and-spring model or to Kuhn's model[11] of rigid, freely jointed segments. In fact, in our case the (exact)[8] mean-square equilibrium distances as well as the intramolecular elastic forces depend on the configurational properties in a less simple way; they are both derivable from the function $C(q)$, which is a generalization of the usual characteristic ratio C_∞ for Fourier modes containing $2\pi/q$ chain atoms within their wavelength.[7,8]

In the two following sections of the present work, this approach will be extended to the case where the monomeric units comprise two skeletal atoms, instead of one only, and also the chain displays a random sequence of stereoisomeric centers (i.e., the phenyl-substituted backbone atoms), as in atactic polystyrene; provided the chain motions are not very localized, we will show that the problem may be reduced to that of an effective chain with a simple $-[A]_N-$ structure. Then, in addition to the intramolecular equilibrium forces embodied in the $C(q)$ function, we will take into consideration the following factors, not appearing in the current Rouse-like[12] or Zimm-like[13] approaches: (i) the internal viscosity; (ii) the hydrodynamic interaction without reaching the Zimm limit; (iii) the good-solvent expansion. Factor i will be regarded as due to the skeletal rotational barriers hindering propagation of intramolecular strain, and it will be assumed to be compounded with the solvent viscosity, in Kramer's diffusive limit.[9,14] Factor ii will be treated within the preaveraged approximation, by using Edwards and Freed's Fourier-transform approach[15] in the discrete-chain formulation given by Ronca.[6,16] The good-solvent expansion will be taken care of by adopting an approach recently proposed by some of us, based on a self-consistent Gaussian approximation for the interatomic distance distribution function.[10] The specific effect exerted by each of the above three factors will then be compared. Some of the parameters we use in this study (see above points i and ii) are derived from previous work,[9] which partly refers to dynamical-mechanical measurements in very viscous solvents;[17-19] this makes it possible to analyze the validity of Stokes' law of friction over a very wide range of solvent viscosities as well as over different experimental techniques. When calculating the excluded-volume parameter (see (iii)), we relied on the viscosimetric results from polystyrene solutions reported by Nyström and Roots.[20]

It should be stressed that the main reason for adopting the above-quoted theoretical approaches is that they are naturally compatible among themselves, all being based on a Fourier representation of the chain motion.

The reader uninterested in the various steps of the mathematical procedure may perhaps jump directly to the Neutron Scattering Experiments section.

Configurational Potential of an $-[A-B]_N-$ Chain

In analogy with the approach previously followed for chains with an $-[A]_N-$ structure,[7] we shall first obtain the configurational free energy of the unperturbed chain, from which the elastic force appearing in the dynamical equations will be evaluated. Let us refer to the schematic structure in Figure 1, where a ringlike chain is considered for simplicity ($N \to \infty$). It should be stressed that the monomeric units will be assumed as effectively equivalent throughout. As it will be explained in a following section dealing with the characteristic ratio $C(q)$, our configurational description is to be understood as the weighted average over the different sequences of stereoisomeric

† Dipartimento di Chimica del Politecnico.
‡ Imperial College.

0024-9297/84/2217-1253$01.50/0

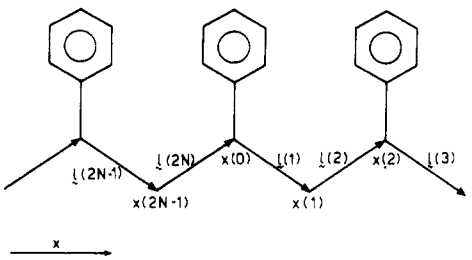

Figure 1. Schematic representation of the polystyrene macromolecule (see text).

centers appearing in a long chain of atactic polystyrene. We define

$$\mathbf{L} = [\mathbf{l}(1), \mathbf{l}(2), \ldots, \mathbf{l}(2N)] \tag{1a}$$

$$\mathbf{M} = \langle \mathbf{L}^{\mathrm{T}} \cdot \mathbf{L} \rangle = \begin{bmatrix} l^2 & \langle \mathbf{l}(1)\cdot\mathbf{l}(2)\rangle & \ldots & \langle \mathbf{l}(1)\cdot\mathbf{l}(2N)\rangle \\ \langle \mathbf{l}(2)\cdot\mathbf{l}(1)\rangle & l^2 & \ldots & \langle \mathbf{l}(2)\cdot\mathbf{l}(2N)\rangle \\ \ldots & & & \\ \langle \mathbf{l}(2N)\cdot\mathbf{l}(1)\rangle & \langle \mathbf{l}(2N)\cdot\mathbf{l}(2)\rangle & \ldots & l^2 \end{bmatrix} \tag{1b}$$

where $\mathbf{l}(k)$ is the vector associated with the kth bond, l is its length, and the angular brackets denote the configurational average. It should be pointed out that, because of the cyclic chain structure, $\mathbf{M}$ is cyclic with order 2; i.e., the kth row is obtained from the $(k-2)$th one after a cyclic shift. Consequently, $\mathbf{M}$ may be made diagonal as follows

$$\mathbf{M} = \mathbf{V}^{-1}\Lambda\mathbf{V} \tag{2a}$$

$$\Lambda = l^2 \begin{bmatrix} \lambda_1 & \cdots & \cdots & 0 \\ & \mu_1 & & \\ & & \lambda_2 & \\ & & & \mu_2 \\ & & & \ddots \\ 0 & & & \ddots \end{bmatrix} \tag{2b}$$

where

$$\mathbf{V} = \begin{bmatrix} \begin{bmatrix} a_1 & b_1 \\ c_1 & d_1 \end{bmatrix} & \cdots & 0 \\ & \begin{bmatrix} a_2 & b_2 \\ c_2 & d_2 \end{bmatrix} & \\ & & \ddots \\ 0 & \cdots & \begin{bmatrix} a_N & b_N \\ c_N & d_N \end{bmatrix} \end{bmatrix} \cdot \times \begin{bmatrix} \mathbf{E}_2 \exp(iq_1) & \mathbf{E}_2 \exp(2iq_1)\cdots \\ \mathbf{E}_2 \exp(2iq_1) & \mathbf{E}_2 \exp(4iq_1)\cdots \\ \mathbf{E}_2 \exp(3iq_1) & \mathbf{E}_2 \exp(6iq_1)\cdots \\ \cdots & \end{bmatrix} \tag{3}$$

$\mathbf{E}_2$ is the unit matrix of order 2 and $q_1 = 2\pi/N$. With standard algebraic methods, we get from the above ($a_n \equiv a(q)$, $b_n \equiv b(q)$, ..., $\lambda_n \equiv \lambda(q)$, etc., with $q \equiv nq_1$)

$$\{q\} = 2\pi/N, 4\pi/N, 6\pi/N, \ldots, 2\pi \tag{4a}$$

$$\lambda(q) \equiv \mathcal{A}(q) + |\mathcal{B}(q)| \tag{4b}$$

$$\mu(q) = \mathcal{A}(q) - |\mathcal{B}(q)| \tag{4c}$$

$$\mathcal{A}(q) = l^{-2}\sum_{\mu=1}^{N} \langle \mathbf{l}(1)\cdot\mathbf{l}(1+2\mu)\rangle \exp(-i\mu q) \tag{4d}$$

$$\mathcal{B}(q) = |\mathcal{B}(q)| \exp[i\Delta(q)] = l^{-2}\sum_{\mu=1}^{N} \langle \mathbf{l}(2)\cdot\mathbf{l}(1+2\mu)\rangle \exp(-i\mu q) \tag{4e}$$

$$a(q) = c(q) = (2N)^{-1/2} \exp[i\Delta(q)/2] \tag{4f}$$

$$b(q) = -d(q) = (2N)^{-1/2} \exp[-i\Delta(q)/2] \tag{4g}$$

where eq 4e defines $\Delta(q)$. The statistically independent bond–vector combinations are

$$\tilde{\mathbf{L}} = \mathbf{L}\mathbf{V}^{\mathrm{T}} \qquad (\mathbf{V}^{-1} = (\mathbf{V}^*)^{\mathrm{T}}) \tag{5}$$

because (see eq 1 and 2)

$$\langle \tilde{\mathbf{L}}^{\mathrm{T}}\cdot\tilde{\mathbf{L}}\rangle = \mathbf{V}\cdot\mathbf{M}\cdot\mathbf{V}^{-1} = \Lambda \tag{5'}$$

(It should be noted that the tilde does not imply the "transpose" operation, which is specified here by a superscript T.) After multiplication by $(2N)^{1/2}$, the odd and even elements of $\tilde{\mathbf{L}}$ ($\tilde{\mathbf{l}}_{\mathrm{A}}$ and $\tilde{\mathbf{l}}_{\mathrm{B}}$, respectively) become

$$\tilde{\mathbf{l}}_{\mathrm{A}}(q) = \sum_{\mu=1}^{N} \exp(i\mu q)\{\exp[i\Delta(q)/2]\mathbf{l}(2\mu-1) + \exp[-i\Delta(q)/2]\mathbf{l}(2\mu)\} \tag{6a}$$

$$\tilde{\mathbf{l}}_{\mathrm{B}}(q) = \sum_{\mu=1}^{N} \exp(i\mu q)\{\exp[i\Delta(q)/2]\mathbf{l}(2\mu-1) - \exp[-i\Delta(q)/2]\mathbf{l}(2\mu)\} \tag{6b}$$

the index $2n-1$ or $2n$ of the general element of $\mathbf{L}$ being related with q through $n = q/(2\pi/N)$. Following ref 7, within the quadratic approximation the configurational free energy of the chain subjected to a set of constant forces producing as an average the configurational components $\tilde{\mathbf{l}}_{\mathrm{A}}(q)$ and $\tilde{\mathbf{l}}_{\mathrm{B}}(q)$ is

$$A\{\tilde{\mathbf{l}}_{\mathrm{A}}(q),\tilde{\mathbf{l}}_{\mathrm{B}}(q)\} = A_0 + \frac{3k_{\mathrm{B}}T}{4Nl^2}\sum_{\{q\}}\{\tilde{\mathbf{l}}_{\mathrm{A}}(q)\cdot\tilde{\mathbf{l}}_{\mathrm{A}}^*(q)/\lambda(q) + \tilde{\mathbf{l}}_{\mathrm{B}}(q)\cdot\tilde{\mathbf{l}}_{\mathrm{B}}^*(q)/\mu(q)\} \tag{7}$$

It should be pointed out that in the present case the eigenvalue functions $\lambda(q)$ and $\mu(q)$ taken together correspond to the generalized characteristic ratio $C(q)$ of an $-[\mathrm{A}]_N-$ polymer.[7] With $\Delta(q)$ they contain complete information on the equilibrium mean-square interatomic distances. As an example, if $r(2m)$ is the distance between the two even or odd atoms of mth neighboring monomeric units, it may be proven that (see Figure 1; the index $2m$ refers to the number of intervening bonds and the suffix zero to the unperturbed state)

$$\langle r^2(2m)\rangle_0 = \frac{l^2}{N}\sum_{\{q\}}\left\{\frac{1-\cos(mq)}{1-\cos q} \times [\lambda(q)(1+\cos\varphi(q)) + \mu(q)(1-\cos\varphi(q))]\right\} \tag{8}$$

where $\varphi(q) = \Delta(q)$ for even and $\varphi(q) = q + \Delta(q)$ for odd atoms.

Dynamic Equations in the Free-Draining Model

Deferring to a later section the explicit evaluation of $\lambda(q)$, $\mu(q)$, and $\Delta(q)$, we may now obtain the x-projection $f_x(k)$ of the elastic force acting on the kth chain atom for a given set of the Fourier components $\{\tilde{\mathbf{l}}_{\mathrm{A}}(q), \tilde{\mathbf{l}}_{\mathrm{B}}(q)\}$. Indicating with $\tilde{l}_{\mathrm{Ax}}$, $\tilde{l}_{\mathrm{Bx}}$ the projection of $\tilde{\mathbf{l}}_{\mathrm{A}}(q)$, $\tilde{\mathbf{l}}_{\mathrm{B}}(q)$, let us write as implicit definitions of $\tilde{x}_{\mathrm{A}}(q)$, $\tilde{x}_{\mathrm{B}}(q)$ ($q \neq 0$)

$$\tilde{l}_{\mathrm{Ax}}(q) = \tfrac{1}{2}[1-\exp(iq)] \times \{\tilde{x}_{\mathrm{A}}(q)\exp[i\Delta(q)/2] + \tilde{x}_{\mathrm{B}}(q)\exp[-i\Delta(q)/2]\} \tag{9a}$$

$$\tilde{l}_{\mathrm{Bx}}(q) = \tfrac{1}{2}[1-\exp(iq)] \times \{\tilde{x}_{\mathrm{A}}(q)\exp[i\Delta(q)/2] - \tilde{x}_{\mathrm{B}}(q)\exp[-i\Delta(q)/2]\} \tag{9b}$$

Remembering that $l_x(k) = x(k) - x(k-1)$ (see Figure 1), eq 6 and 9 establish a connection between $\tilde{x}_A(q)$, $\tilde{x}_B(q)$, and $x(k)$, which is explicitly reported in eq A-4 of the Appendix. Expressing now the scalar products in eq 7 as a sum of separate contributions over x, y, z, we have

$$f_x(k) = -\sum_{j=A,B}\sum_{\{q\}} \frac{\partial A}{\partial \tilde{l}_{jx}(q)}\left[\frac{\partial \tilde{l}_{jx}(q)}{\partial l_x(k)} - \frac{\partial \tilde{l}_{jx}(q)}{\partial l_x(k+1)}\right] \quad (10)$$

while the full expression is reported in the Appendix (eq A-1). Introducing the time variable, denoting with ζ_1 and ζ_2 the effective solvent-friction coefficients of the even- and odd-numbered chain atoms (see Figure 1), and omitting initially the excluded-volume effect as well as the hydrodynamic interaction and the internal viscosity, the dynamic equations are

$$-f_x(2\mu - 1,t) + \zeta_1 \dot{x}(2\mu - 1,t) = X_1(\mu,t) \quad (11a)$$

$$-f_x(2\mu,t) + \zeta_2 \dot{x}(2\mu,t) = X_2(\mu,t) \quad (11b)$$

where X_1 and X_2 are the stochastic Brownian forces associated with the two atoms of the μth monomeric unit. Multiplying by $\exp(i\mu q)$ and summing over μ from 1 to N remembering eq A-4, we have a system of two linear first-order differential equations containing $\tilde{x}_A(q,t)$ and $\tilde{x}_B(q,t)$ (see eq A-8). The only physically meaningful solution is given by

$$\tilde{x}_A(q,t) = \int_{-\infty}^{t}\left[\rho_1(q,t')\exp\left[-\frac{t-t'}{\tau_1(q)}\right] + \rho_2(q,t')\exp\left[-\frac{t-t'}{\tau_2(q)}\right]\right]dt' \quad (12a)$$

$$\tilde{x}_B(q,t) = \int_{-\infty}^{t}\left[\sigma_1(q,t')\exp\left[-\frac{t-t'}{\tau_1(q)}\right] + \sigma_2(q,t')\exp\left[-\frac{t-t'}{\tau_2(q)}\right]\right]dt' \quad (12b)$$

where ρ_h and σ_h are linear combinations of the $\tilde{X}_k$. The full expressions of ρ_h, σ_h, $\tau_h(q)$ ($h = 1, 2$) are reported in the Appendix, eq A-11–A-14. Confining ourselves here to motions not involving short chain sequences, so that $q \ll 1$ rad (when $\Delta(q) \ll 1$ rad, cf. eq 4) from (A-11) and (A-12) we get for the relaxation times

$$\tau_1(q) \simeq \frac{2l^2\lambda(q)(\zeta_1 + \zeta_2)}{3k_BTq^2} \quad (13a)$$

$$\tau_2(q) \simeq \frac{l^2\mu(q)\zeta_1\zeta_2}{6k_BT(\zeta_1 + \zeta_2)} \quad (13b)$$

It is natural to recognize $\tau_1(q)$ and $\tau_2(q)$ as the equivalent of the acoustic and of the optical branch in a monodimensional Brillouin zone.[21] Clearly, for sufficiently small q, $\tau_1(q) \gg \tau_2(q)$, the more so because $\lambda(q)$ is expected to be much larger than $\mu(q)$ (see eq 4). This suggests that the contributions given by the latter branch to the chain dynamics may be neglected in the present limit. Considering that eq A-13 gives

$$\lim_{q\to 0}\rho_1 = \lim_{q\to 0}\sigma_1 = [\tilde{X}_1(q,t) + \tilde{X}_2(q,t)]/(\zeta_1 + \zeta_2) \quad (14)$$

let us define

$$\zeta = (\zeta_1 + \zeta_2)/2 \quad (15a)$$

$$\tilde{X}_{AV}(q,t) = [\tilde{X}_1(q,t) + \tilde{X}_2(q,t)]/2 \quad (15b)$$

so that we have from eq 12–15 ($q \ll 1$)

$$\tau_1(q) \simeq \frac{4\lambda(q)t_0}{3q^2} \qquad \left(t_0 = \frac{\zeta l^2}{k_BT}\right) \quad (16a)$$

$$\tilde{x}_A(q,t) \simeq \tilde{x}_B(q,t) \simeq \zeta^{-1}\int_{-\infty}^{t}\tilde{X}_{AV}(q,t')\exp\left[-\frac{t-t'}{\tau_1(q)}\right]dt' \quad (16b)$$

It should be pointed out that the above results are essentially identical with those for an $-[A]_{2N}-$ chain (see eq 25 and 25′ of ref 8) provided we state the equivalence

$$C(q/2) \equiv \lambda(q) \quad (17a)$$

$$\tau(q/2) \equiv \tau_1(q) \quad (17b)$$

$$\tilde{x}(q/2,t) \equiv \tfrac{1}{2}[\tilde{x}_A(q,t) + \tilde{x}_B(q,t)] \quad (17c)$$

$$\tilde{X}(q/2,t) \equiv \tilde{X}_{AV}(q,t) \quad (17d)$$

(The correspondence between q in the $-[A-B]_N-$ chain and $q/2$ in the equivalent $-[A]_{2N}-$ chain may be easily understood if we consider the wavelength of the q mode along the chain contour; this is given by $2\pi/q$ *monomeric units* in the former case, which means twice as many *chain atoms* (i.e., $2\pi/(q/2)$) in the equivalent chain.) We have thus reduced our dynamical problem to that of an equivalent $-[A]_{2N}-$ chain through eq 15–17, at least for sufficiently collective modes (i.e., $q \ll 1$); for simplicity we shall adopt henceforth the corresponding formalism, based on ζ, $C(q)$, $\tau(q)$, $\tilde{x}(q,t)$, and $\tilde{X}(q,t)$.

Solvent and Internal Viscosity Effects

It is now possible to introduce (i) the chain expansion due to the good solvent, (ii) the hydrodynamic interaction, and (iii) the internal viscosity.

(i) Good-Solvent Effect. This will be embodied into the generalized characteristic ratio $C(q)$ (see eq 17) which takes the following "effective" form[10]

$$C_{eff}(q) = C(q)\tilde{\alpha}^2(q) \quad (18)$$

Here $\tilde{\alpha}^2(q)$ is the square expansion factor of the q normal mode which may be evaluated if the excluded volume parameter per chain atom β is known. Since our experimental data were obtained from polystyrene solutions in C_6D_6 and CS_2 at 30 and 70 °C, i.e., much above the Θ temperature, we could not make use of the linear expansion of β in terms of $(T - \Theta)$, as done elsewhere.[22] Instead, we preferred to get an approximate estimate of the solvent effect by using the viscosity plots reported by Nyström and Roots for different solvent types and molecular masses.[20] Classifying our solvents as "good", we first obtained the average expansion factor $\alpha(M)$ from Figure 8 of ref 20 and the relationship

$$\alpha^3(M) = [\eta]_{\text{good solvent}}/[\eta]_{\Theta\text{ solvent}} \quad (19)$$

where M is the molecular mass. From Flory's theory[23] (reported in terms of $\alpha_F^2(k)$ in Figure 1 of ref 10, k being the number of skeletal bonds; $k = M/52$ for polystyrene) we obtained $\bar{\beta}k^{1/2}$, hence $\bar{\beta}$, which is an adimensional form of the excluded volume parameter per chain atom.[10] Taking a typical value of 10^5 for our molecular mass, $\bar{\beta} \simeq 0.016$. With this parameter, and again with the use of Figure 1 of ref 10, we obtained the plot of $\tilde{\alpha}^2(q)$ vs. q reported in Figure 2. Possible differences induced either by the temperature (i.e., 30 or 70 °C) or by the solvent (cf. Table I) were disregarded. The modest expansion effect due to the screened intramolecular interactions, existing even in the Θ state,[24] was also disregarded.

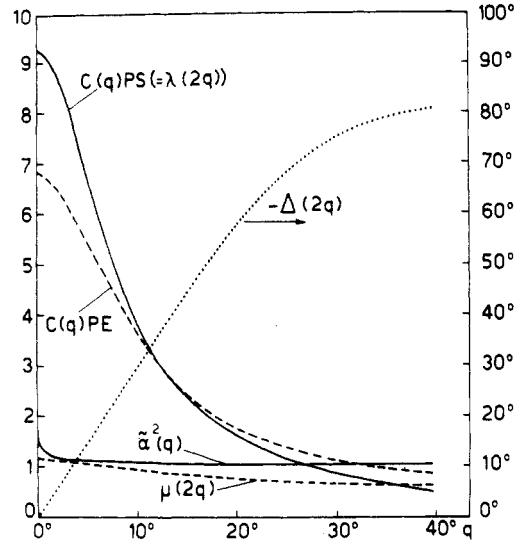

Figure 2. Plots of $C(q)$ for atactic polystyrene at 30 °C (PS, from eq 29) and polyethylene at 127 °C (PE, from ref 7). Also reported for PS are the plots of $\mu(2q)$, $\Delta(2q)$ (from eq 4), and $\tilde{\alpha}^2(q)$ (see text).

(ii) Hydrodynamic Interaction. According to Ronca,[16] the effect of hydrodynamic interaction may be incorporated into a suitable modification of the friction factor, which acquires the following q-dependence[9c]

$$\zeta(q) = \zeta/[1 + h_0 f(q)] \tag{20}$$

where, indicating by $r(k)$ the distance between backbone atoms separated by k bonds[9c]

$$h_0 f(q) = \frac{\zeta}{6\pi\eta_x}\sum_{i,j=1}^{2N}\left\{\frac{1}{2N}\cos[q(i-j)]\langle r^{-1}(|i-j|)\rangle\right\} = \frac{\zeta}{6\pi\eta_s}\sum_{k=1}^{2N}\left\{\frac{2N-k}{N}\cos(qk)\langle r^{-1}(k)\rangle\right\} \tag{20^i}$$

and, according to our Gaussian approximation

$$\langle r^{-1}(k)\rangle = \left(\frac{6}{\pi\langle r^2(k)\rangle}\right)^{1/2} \tag{20^{ii}}$$

If we put $q = 0$ into 20^i it is easy to show that

$$h_0 f(0) = \frac{\zeta}{6\pi\eta_s}\frac{2N}{R_H} \tag{20^{iii}}$$

where R_H is the hydrodynamic radius. For sake of agreement with previous definitions, we will put (the subscript zero stands for the unperturbed average)

$$f(q) = \pi\sqrt{2N}\frac{\sum_{k=1}^{2N}(2N-k)\cos(qk)\langle r^{-1}(k)\rangle}{\sum_{k=1}^{2N}(2N-k)\langle r^{-1}(k)\rangle_0} = \frac{\pi R_{H_0}}{(2N)^{3/2}}\sum_{k=1}^{2N}(2N-k)\cos(qk)\langle r^{-1}(k)\rangle \tag{20^{iv}}$$

and consequently

$$h_0 = \frac{\zeta}{3\pi^2\eta_s}\frac{(2N)^{1/2}}{R_{H_0}} \simeq \frac{4}{9\pi^2}\left(\frac{6}{\pi C(0)}\right)^{1/2}\frac{1}{l}\frac{\zeta}{\eta_s} \qquad (N \gg 1) \tag{20^v}$$

It should be noted that $f(0)$ reduces to $\pi(2N)^{1/2}$ in the unperturbed case (see eq 20^{iv}), like in a previous paper.[9c] It should also be noted that a minor change from Ronca's procedure described in the same paper (see Appendix I of ref 9c) is introduced; namely, the assumption of ring closure is now abandoned.

(iii) Internal Viscosity. Accounting for this factor entails a nontrivial effect on the dynamic equations.[9] Since our attention is confined to the Fourier modes with $q \ll 1$, the observation times may be assumed to be much larger than the average relaxation time for skeletal bond rotations τ_0. Consequently, the symmetrized form of the dynamic equation[25] reduces to ($t \gg \tau_0$)

$$a^2\tilde{x}(q,t) + 2ab\dot{\tilde{x}}(q,t) + (b^2 + c^2\tau_0^2)\ddot{\tilde{x}}(q,t) = a\tilde{X}_\alpha(q,t) + b\dot{\tilde{X}}_\alpha(q,t) - ic\tau_0\dot{\tilde{X}}_\beta(q,t) \tag{21}$$

$$\{q\} = \pm\frac{\pi}{N}, \pm\frac{2\pi}{N}, \ldots \tag{A-7}$$

where ($|q| \ll 1$)

$$a = \frac{3k_BT}{C_{eff}(q)l^2}q^2 \tag{21'a}$$

$$b = \zeta(q) \tag{21'b}$$

$$c = \frac{4k_BT}{C_{eff}(q)l^2}q \tag{21'c}$$

$$\langle\tilde{X}_{\alpha(\beta)}(q,t)\tilde{X}^*_{\alpha(\beta)}(q,0)\rangle = 4Nk_BT\zeta(q)\delta(t) \tag{21'd}$$

$$\langle\tilde{X}_{\alpha(\beta)}(q,t)\tilde{X}^*_{\beta(\alpha)}(q,0)\rangle = \frac{8iN(k_BT)^2}{C_{eff}(q)l^2}q\cdot\tau_0\delta(t) \tag{21'e}$$

From the above, the interatomic correlation function becomes (see eq 42 of ref 9c)

$$B(k,t) = \langle(\mathbf{r}(k,t) - \mathbf{r}(0,0))^2\rangle = 3\langle[x(k,t) - x(0,0)]^2\rangle = \frac{l^2}{2N}\sum_{|q|}\frac{2C_{eff}(q)}{q^2}\left\{1 - e^{-t/\bar{\tau}(q)}\cos(qk)\cos\left[\gamma(q)\frac{t}{\bar{\tau}(q)}\right]\right\} \tag{22}$$

where $\mathbf{r}(k,t)$ is the vector position of the kth atom at time t, and

$$\bar{\tau}(q) \simeq t_0\left\{\frac{C_{eff}(q)}{3q^2}\frac{1}{1 + h_0 f(q)} + \frac{8}{3}\frac{2}{C_{eff}(q)}[1 + h_0 f(q)]\left(\frac{\tau_0}{t_0}\right)^2\right\} \tag{22'a}$$

$$\gamma(q) = \frac{4\tau_0}{t_0}\frac{1 + h_0 f(q)}{C_{eff}(q)}q \tag{22'b}$$

(In eq 22 the term with $q = 0$ is easily obtained analytically as the limit for $q \to 0$.) Since the interatomic vector $\mathbf{r}(k)$ is nothing but $[\mathbf{r}(k,0) - \mathbf{r}(0,0)]$, we have

$$\langle r^2(k)\rangle = B(k,0) \tag{22''}$$

which completes the operational definition of $\langle r^{-1}(k)\rangle$ (see eq 20^{ii}). Clearly, the effective relaxation time $\bar{\tau}(q)$ reduces to $\tau(q)$ (see eq 17) if the internal viscosity, the hydrodynamic interaction, and the excluded-volume effect are absent, i.e., $\tau_0 \equiv 0$, $h_0 \equiv 0$, $\tilde{\alpha}^2(q) \equiv 1$.

Once we have the correlation function $B(k,t)$ (see eq 22) the dynamic structure factor may be evaluated (see following eq 32). To get $B(k,t)$, we must select appropriate values of ζ, τ_0, and h_0 (see eq 15, 21, and 20, respectively) for each temperature. The first two parameters will be expressed as

$$\zeta = 6\pi R_{eff}\eta_s \tag{23}$$

$$\tau_0 = K\eta_s\exp(\Delta/k_BT) \tag{24}$$

where Δ is the effective average energy barrier between

Table I
Sample Characteristics

sample	sample no.	exptl technique (Q, Å^{-1})	temp, °C	M_w	solvent	concn, wt %
polystyrene (hydrogenated)	1a	spin echo ($Q < 0.06$)	30	95 000	C_6D_6	3
	1b	spin echo ($Q > 0.06$)	30	50 000	C_6D_6	3
	2	spin echo ($0.05 < Q < 0.13$)	70	95 000	C_6D_6	3
polystyrene (deuterated)	3	spin echo ($0.04 < Q < 0.13$)	30	76 000	CS_2	2
	4	back-scattering ($0.11 < Q < 0.27$)	30	100 000	CS_2	3

Table II
Physical Parameters Used in the Calculations

symbol	definition[a]	value	source
l	C–C bond length	1.54 Å	current literature
ϑ	∠C–C–C bond angle	112°	current literature
Δ	eq 24	3.7 kcal/mol	theory, ref 26
h_0	eq 20	0.03	best fit with mechanical results (ref 9c, 17–19)
$\bar{\beta}$	eq 10, 17 of ref 10	0.016	present paper, section containing eq 18, 19
R_{eff}	eq 23	0.38 ± 0.06 Å	present paper, best fit with scattering results
$2N$	no. of skeletal atoms, eq 4	2000	same order of magnitude as the experimental M_w (see Table I)
η_s	solvent viscosity	0.60×10^{-2} P (C_6D_6, 30 °C), 0.35×10^{-2} P (CS_2, 30 °C), 0.366×10^{-2} P (C_6D_6, 70 °C)	current literature
ζ	eq 15	$(4.3 \pm 0.7) \times 10^{-10}$ g s^{-1} (C_6D_6, 30 °C), $(2.5 \pm 0.4) \times 10^{-10}$ g s^{-1} (CS_2, 30 °C), $(2.6 \pm 0.4) \times 10^{-10}$ g s^{-1} (C_6D_6, 70 °C)	from eq 23
t_0	eq 16	$(2.4 \pm 0.4) \times 10^{-12}$ s (C_6D_6, 30 °C), $(1.4 \pm 0.2) \times 10^{-12}$ s (CS_2, 30 °C), $(1.3 \pm 0.2) \times 10^{-12}$ s (C_6D_6, 70 °C)	from eq 16
τ_0	eq 21	$(1.1 \pm 0.2) \times 10^{-10}$ s (C_6D_6, 30 °C), $(0.66 \pm 0.11) \times 10^{-10}$ s (CS_2, 30 °C), $(0.34 \pm 0.06) \times 10^{-10}$ s (C_6D_6, 70 °C)	best fit with mechanical results (ref 9c, 17–19)

[a] Definition or first appearance in equations.

rotational states and K is a proportionality constant.[9] In (23) we assume the validity of Stokes' law with a suitable effective radius per chain atom, while in (24) the rotational relaxation process is taken to be of the Kramers' activated type in the large-viscosity limit (see, e.g., eq 17 of ref 14, where $r \propto \tau_0^{-1}$). The corresponding expression given by one of the present authors (see eq 22 of ref 9b) may be put into agreement with the above if the frequency factor A is taken as $\propto \eta_s^{-1}$, following Kramers' ideas. Equations 23 and 24 contain three parameters which cannot be exactly deduced from theoretical considerations, i.e., R_{eff}, K, and Δ. The last of these may be approximately derived from the calculated energy maps of Yoon et al.,[26] considering Helfand's conclusions[27] (supported by Fixman's numerical calculations[28]) that the effective rotational barrier for the chain is close to the value pertaining to single skeletal bonds. Accordingly, we have chosen $\Delta \simeq 3.7$ kcal/mol. Also, from previous comparison of the calculated complex modulus of polystyrene chains with dynamical-mechanical results of the Wisconsin group,[17-19] the best-fitting value of τ_0 at $T = 30$ °C turns out to be close to $47\zeta l^2/k_B T$, whence $K = 5.7 \times 10^{-4}\zeta/\eta_s$ cm. This leaves a single parameter to be adjusted, e.g., R_{eff}, from which ζ may be obtained for a given solvent. Although at this point we might use the relationship between h_0 and ζ/η_s established through the preaveraged Oseen tensor (see eq 20^v), we have chosen to keep h_0 fixed at the empirical value 0.03 which was adopted to fit the dynamical-mechanical results,[9c] in good agreement with the figures repeatedly obtained by the Wisconsin group.[17-19] The reason for this choice is that eq 20^v is due to a rather elaborate sequence of theoretical assumptions.

We have chosen $2N = 2000$ for our calculations, corresponding to $M \simeq 10^5$ which is close to the experimental M_w's (see Table I). No particular accuracy appears to be required for this figure, considering that in our Q range the dynamic structure factor is independent of M, as long as the radiation probes internal motions only.

The basic physical parameters adopted in our calculations are listed in Table II; some of these values will be commented upon in a following section. Before proceeding to evaluate the dynamic structure factor, we still have to account for the chain configurational properties, incorporated in the function $C(q)$ (see eq 17). Its calculation for an atactic polystyrene chain will be discussed in the next section.

Evaluation of $C(q)$ for Atactic Polystyrene

In analogy with the procedure followed by some of us to evaluate C_∞ for atactic polypropylene, we will adopt the pseudostereochemical equilibrium method,[29] thus formally reducing the problem to that of a chain with the same structure for all its monomeric units. Following Yoon, Sundararajan, and Flory[26] the rotational-isomeric-state scheme will be adopted, with two possible rotations around each skeletal bond and by assuming first-neighbor energy correlation. Let us label with m (meso) and r (racemic) respectively the pairs of adjacent monomeric units (dyads) with the same and with an opposite stereochemical configuration for their substituted C atoms. We shall denote with $\mathbf{U}_m$ and $\mathbf{U}_r$ the 2×2 matrices carrying the statistical weights for the allowed rotation pairs around bonds $(2\mu - 1, 2\mu)$ for either dyad, and with $\mathbf{U}_1$ the corresponding, undifferentiated matrix for the rotation pair $(2\mu, 2\mu + 1)$

(see Figure 1). Let us define

$$\mathbf{U}' = \begin{bmatrix} \mathbf{U}_1 & \mathbf{0} \\ \mathbf{0} & \mathbf{U}_1 \end{bmatrix} \tag{25a}$$

$$\mathbf{U}'' = \begin{bmatrix} \sigma\mathbf{U}_m & \mathbf{U}_r \\ \mathbf{U}_r & \sigma\mathbf{U}_m \end{bmatrix} \tag{25b}$$

$$\lambda = \text{largest eigenvalue of } \mathbf{U} = \mathbf{U}''\cdot\mathbf{U}' \tag{25c}$$

$$\mathbf{a}\ (\mathbf{a}^*) = \text{row (column) eigenvector of U, for the eigenvalue } \lambda \tag{25d}$$

$$(\mathbf{U}_3', \mathbf{U}_3'', \mathbf{a}_3, \mathbf{a}_3^*) = (\mathbf{U}', \mathbf{U}'', \mathbf{a}, \mathbf{a}^*) \otimes \mathbf{E}_3 \tag{25e}$$

$$\Psi_1 = \begin{bmatrix} \Psi+ & \mathbf{0} \\ \mathbf{0} & \Psi- \end{bmatrix} \tag{25f}$$

$$\Psi_2 = \begin{bmatrix} \Psi- & \mathbf{0} \\ \mathbf{0} & \Psi+ \end{bmatrix} \tag{25g}$$

$$\Psi\pm = \begin{bmatrix} \mathbf{T}(\pm\varphi_1) & \mathbf{0} \\ \mathbf{0} & \mathbf{T}(\pm\varphi_2) \end{bmatrix} \tag{25h}$$

$$\mathbf{Z} = \mathbf{U}_3''\Psi_2\mathbf{U}_3'/\lambda \tag{25i}$$

$$\tau = \Psi_1\mathbf{Z} \tag{25j}$$

In the above, σ is a suitable multiplier that adjusts the percentage of meso dyads at the value required,[29] $\otimes$ is the symbol of the matrix direct product and $\mathbf{E}_3$ is the unit matrix of order 3. $\mathbf{T}(\varphi)$ is the (3 × 3) matrix performing the rotation φ around the general bond. For $\mathbf{U}_m$, $\mathbf{U}_r$, and $\mathbf{U}_1$ we used the same structure and same parameters as adopted by the quoted authors, i.e.,

$$\mathbf{U}_m = \begin{bmatrix} \omega'' & \eta^{-1} \\ \eta^{-1} & \omega/\eta^2 \end{bmatrix} \tag{26a}$$

$$\mathbf{U}_r = \begin{bmatrix} 1 & \omega'/\eta \\ \omega'/\eta & \eta^{-2} \end{bmatrix} \tag{26b}$$

$$\mathbf{U}_1 = \begin{bmatrix} 1 & 1 \\ 1 & 0 \end{bmatrix} \tag{27c}$$

$$\omega \simeq \omega' \simeq 1.3\exp(-1000/T) \tag{26d}$$

$$\omega'' \simeq 1.8\exp(-1100/T) \tag{26e}$$

$$\eta \simeq 0.8\exp(200/T) \tag{26f}$$

Correspondingly, $\varphi_1 \simeq +10°$ and $\varphi_2 \simeq +110°$,[26] while (ϑ = ∠C–C–C)

$$\mathbf{T}(\varphi) = \begin{bmatrix} -\cos\vartheta & \sin\vartheta & 0 \\ \sin\vartheta\cos\varphi & \cos\vartheta\cos\varphi & \sin\varphi \\ \sin\vartheta\sin\varphi & \cos\vartheta\sin\varphi & -\cos\varphi \end{bmatrix} \tag{27}$$

in the assumption that $\varphi = 0°$ denotes the trans arrangement and the bond undergoing rotation coincides with the x-axis of its intrinsic Cartesian frame. The angle ϑ was equated to 112° on both the skeletal atoms of the monomeric unit.

Using current matrix algebra, from eq 25–27 it may be shown that

$$\langle \mathbf{l}(1)\cdot\mathbf{l}(1+2\mu)\rangle = l^2[1\ 0\ 0]\mathbf{a}_3\tau^{|\mu|}\mathbf{a}_3^*\begin{bmatrix}1\\0\\0\end{bmatrix};\ -\infty < \mu < \infty \tag{28a}$$

$$l^2[1\ 0\ 0]\mathbf{a}_3\mathbf{Z}\tau^{\mu-1}\mathbf{a}_3^*\begin{bmatrix}1\\0\\0\end{bmatrix};\ \mu \geq 1 \tag{28b}$$

$$\langle \mathbf{l}(2)\cdot\mathbf{l}(1+2\mu)\rangle = \nearrow \quad \searrow$$

$$l^2[1\ 0\ 0]\mathbf{a}_3\tau^{-\mu}\Psi_1\mathbf{a}_3^*\begin{bmatrix}1\\0\\0\end{bmatrix};\ \mu \leq 0 \tag{28c}$$

where the periodic chain structure is implicit ($\mathbf{l}_k \equiv \mathbf{l}_{2N+k}$). From eq 4, 25, and 28 we have

$$C(q) = \lambda(2q) = \mathcal{A}(2q) + |\mathcal{B}(2q)| \tag{29a}$$

$$\mathcal{A}(2q) = [1\ 0\ 0]\mathbf{a}_3(\mathbf{E} - \tau^2)\Phi\mathbf{a}_3^*\begin{bmatrix}1\\0\\0\end{bmatrix} \tag{29b}$$

$$\mathcal{B}(2q) = [1\ 0\ 0]\mathbf{a}_3\{[\mathbf{E} - \tau\exp(-2iq)]\Phi\Psi_1 + \mathbf{Z}\Phi[\mathbf{E}\exp(-2iq) - \tau]\}\mathbf{a}_3^*\begin{bmatrix}1\\0\\0\end{bmatrix} \tag{29c}$$

$$\Phi = [\mathbf{E} + \tau^2 - 2\cos(2q)\tau]^{-1} \tag{29d}$$

$\mathbf{E}$ being the unit matrix of the same order as τ. Taking T = 303 K and σ = 1, the fraction of meso dyads, f_m

$$f_m = \frac{\sigma}{\lambda}\mathbf{a}\begin{bmatrix}\mathbf{U}_m & \mathbf{0} \\ \mathbf{0} & \mathbf{U}_m\end{bmatrix}\mathbf{a}^* \tag{30}$$

is 0.43, and correspondingly for racemic dyads f_r = 0.57. The statistical distribution of the dyads implicit in our description has been verified to be close to Bernoullian, or zero-order Markoffian.[29] It should be remarked that by choosing σ = 1 we have actually referred to the same ensemble of polystyrene chains as obtained from a hypothetical stereochemical equilibration.[30] Figure 2 shows the resulting function $C(q)$ in a range of q values extending from the cooperative chain modes ($q \simeq 0$) to quite localized modes with $n_q = 2\pi/q \simeq 10$ chain atoms per wavelength. For comparison, the $\mu(2q)$ function is also reported, thus enabling evaluation of both $\tau_1(q)$ and $\tau_2(q)$ (see eq 13); it is easy to check that $\tau_1(q) \gg \tau_2(q)$ over the whole range for any value of ζ_1 and ζ_2, is agreement with the initial hypothesis. Also for comparison, $C(q)$ previously obtained by one of us for polyethylene[7] is shown; the greater chain rigidity of polystyrene shows up both in the larger peak value and in the smaller half-peak width, the product of the two parameters being roughly the same for the two polymers. As may be observed in Figure 2, the sharpness of the peak at the origin is further enhanced after multiplying $C(q)$ by the square expansion factor $\tilde{\alpha}^2(q)$ (see eq 18). For computational purposes, the function has been approximated to the expression

$$C(q) \simeq \frac{0.0899}{1 - 0.990\cos q} + 0.365 \simeq \frac{0.0899}{0.010 + 0.495q^2} + 0.365 \tag{31}$$

as previously done by some of us.[8,24] The last approximate equality is justified by the present assumption of small $|q|$. We may roughly take 30°, or $2\pi/12$, as the upper limit of validity of the present approach, corresponding to configurational waves of not less than ~12 chain atoms per

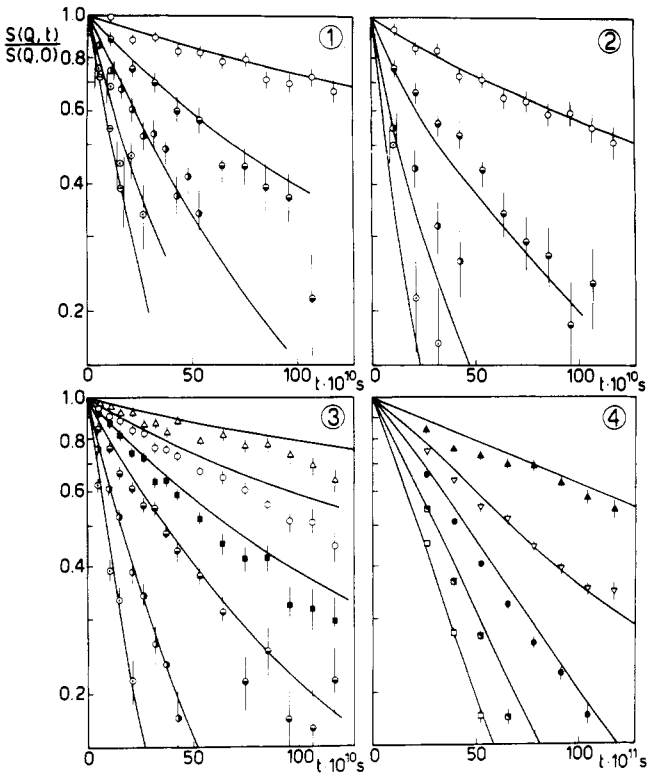

Figure 3. Experimental points (with error bars) and calculated plots of $S_{coh}(Q,t)$ (eq 32) vs. t for different Q values. Sections 1, 2, 3 and 4 respectively correspond to samples 1–4 reported in Table I. Data from back-scattering experiments (sample 4) do not comprise the results for the shortest time, in view of the large error involved with data processing.[34] The Q-values (Å^{-1}) for sections 1–3 are as follows: (△) 0.0396; (○) 0.0528; (■) 0.0660; (◒) 0.0792; (◑) 0.1056; (⊙) 0.1320; (⊖) 0.1583. Those for section 4 are as follows: (▲) 0.11; (▽) 0.15; (●) 0.19; (◨) 0.23; (□) 0.27.

wavelength, a distance of observation corresponding to just a few angstroms. The modest effect on $C(q)$ of the change of temperature from 30 to 70 °C will be disregarded in the following.

Neutron Scattering Experiments

The data were obtained by using two high-resolution spectrometers at the Institut Laue-Langevin;[31] they are reported in Figure 3.

The dynamic coherent structure factor $S(Q,t)$ was obtained directly for polystyrene in C_6D_6 by using the IN11 spin-echo spectrometer.[32,33] Because the measurement keeps track of the neutron spin, this spectrometer allows clean separation of the coherent and incoherent signals. Details of the narrow molecular weight polystyrene fractions and the solution concentrations are given in Table I; samples 1a and 1b differ in their molecular weight only. All the samples were held in quartz cells for ambient temperature experiments and niobium cells at higher temperature. Data at 30 °C for the lower molecular weight sample have been reported previously[4] together with the details of the experiments. The new data were obtained in exactly the same way.

With the IN10 back-scattering spectrometer the dynamic scattering was measured initially as the frequency transform of $S(Q,t)$, $S(Q,\omega)$.[34] This instrument has a limiting energy resolution of 1 μeV and a lowest measuring angle corresponding to $Q = 0.07$ Å^{-1}. In this case we include data for $Q > 0.11$ Å^{-1}, where the full width at half-maximum of $S(Q,\omega)$ becomes greater than the energy spread of the incident neutrons.

The details of the measurements on solutions, held in thin-walled aluminum cans, have been reported previously.[3] In principle, the back-scattering signal is a sum of coherent and incoherent contributions. In our case the only sample examined with this technique is a deuterated polymer (see Table I, sample 4) in CS_2, for which the incoherent contribution is almost negligible.[2] The data were previously analyzed in the form of $S(Q,\omega)$. For the present purposes the frequency data have been Fourier transformed to give $S(Q,t)$ to enable comparison with the calculated correlation functions. A discussion of the relationship between $S(Q,t)$ and $S(Q,\omega)$ is given by Heidemann et al.[34] The procedure adopted for obtaining $S(Q,t)$ from IN10 data is given in a report by W. S. Howells.[35] Data are first corrected for can scattering, self-absorption, etc. in the usual way. A fast Fourier transform of the sample and resolution experiments is made and the sample $S(Q,t)$ is obtained by dividing the two FT spectra. The standard deviations are computed for the Fourier coefficients from the statistical noise on the original data. The function $S(Q,t)/S(Q,0)$ should be unity at $t \doteq 0$ so the data have been renormalized using visual extrapolation to obtain $S(Q,0)$.

In conclusion, all our measurements concern *coherent* scattering (see Figure 3). The computed curves have been fitted to the experimental scattering without further adjustment.

Results and Discussion

The dynamic, coherent structure factor of the N-monomeric units polystyrene chain may be expressed as follows[36]

$$S_{coh}(Q,t) = (2N)^{-1}\left\{\exp\left[-\frac{1}{6}Q^2B(0,t)\right] + 2\sum_{k=1}^{2N}\left(1 - \frac{k}{2N}\right)\exp\left[-\frac{1}{6}Q^2B(k,t)\right]\right\} \quad (32)$$

where *it is assumed for simplicity that the total effective scattering power is evenly concentrated on the chain atoms* ($Q = 4\pi \sin(\vartheta/2)/\lambda$).[37] First the correlation function $B(k,t)$ has been evaluated by using eq 22, with the physical parameters of Table II and the function $C(q)$ given by eq 31 (and reported in Figure 2). The resulting plots of $S(Q,t)$ vs. t are given in Figure 3 for all the samples of Table I. All the experimental values have been considered; as the figure shows, comparison with the experimental results appears to be reasonably good, the more so because our calculations have been fitted with a single parameter.

To summarize the dependence of the dynamic scattering results on the reciprocal coordinate Q, we have chosen the half-peak time $t_{1/2}$ (i.e., $S(Q,t_{1/2}) = {}^1/_2S(Q,0)$) as the characteristic parameter. (The reason for our preferring $t_{1/2}$ to Ω^{-1}, where $\Omega = [\partial \ln S(Q,t)/\partial t]_{t=0}$, is twofold. On the one hand, $t_{1/2}$ accounts for some intermediate relaxation of $S(Q,t)$, unlike Ω which only describes the initial relaxation; incidentally, for $t \to 0$ the internal viscosity has no effect;[9c] second, $t_{1/2}$ is less strongly affected than Ω by the uncertainty in the determination of $S(Q,0)$, which in the back-scattering technique is inevitably entailed by the Fourier transform procedure.) The plots of $t_{1/2}$ vs. Q are reported in Figure 4. It should be observed that our samples are represented by three curves only, from a computational viewpoint, since both CS_2 solutions at 30 °C produce the same coherent structure factor for a given Q, whether they are examined with the spin-echo or with the back-scattering technique (see Table I). The $t_{1/2}$ vs. Q dependence is conveniently expressed in terms of the approximate power law

$$t_{1/2}Q^{\mathcal{B}} \cong \text{const} \quad (33)$$

Table III

(a) Average Power-Law Exponent $\mathcal{B}^a$ in $t_{1/2}Q^{\mathcal{B}}$ = const for Different Ranges of Q

T = 30 °C		T = 70 °C	
calcd	exptl	calcd	exptl
2.86 [0.05 < Q < 0.15 Å^{-1}]	2.6 ± 0.2 [0.07 < Q < 0.16 Å^{-1}] (in C_6D_6)	2.98 [0.05 < Q < 0.16 Å^{-1}]	2.9 ± 0.2 [0.05 < Q < 0.13 Å^{-1}] (in C_6D_6)
	2.7 ± 0.2 [0.05 < Q < 0.13 Å^{-1}] (in CS_2, spin echo)		
2.15 [0.15 < Q < 0.30 Å^{-1}]	2.0 ± 0.2 [0.11 < Q < 0.27 Å^{-1}] (in CS_2, back-scattering)		

(b) Variation $\Delta\mathcal{B}$ Induced upon the Calculated Average Exponent $\mathcal{B}^a$ by the Change of Physical Parameters Indicated on Top of Each Column (T = 30 °C)

range	suppression of good-solvent expansion[b]	suppression of hydrodynamic interaction[c]	suppression of internal viscosity[d]
0.05 < Q < 0.11 Å^{-1}	+0.2	+0.9	+0.5
0.11 < Q < 0.19 Å^{-1}	+0.1	+0.3	+0.4
0.19 < Q < 0.30 Å^{-1}	~0	0 to +0.1	+0.4

[a] Coherent scattering; see eq 33. [b] That is, $\tilde{\alpha}^2(q) \equiv 1$, eq 18. [c] That is, $h_0 = 0$, eq 20–22′. [d] That is, $\tau_0 = 0$, eq 21–22′.

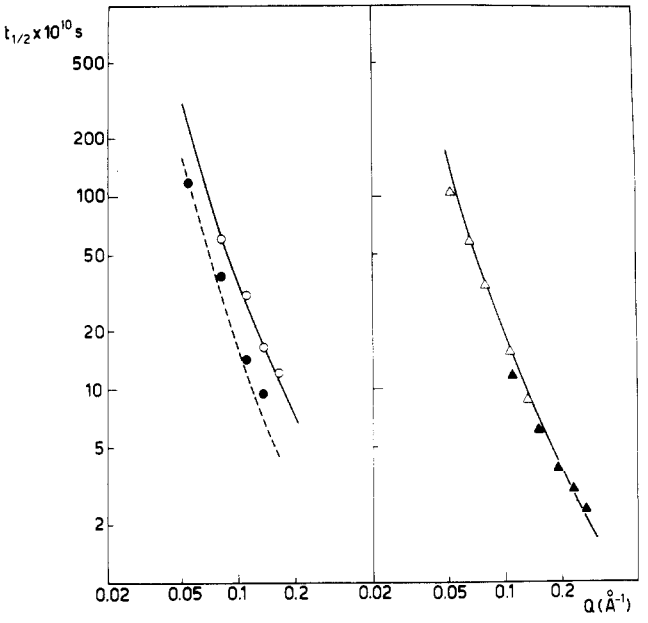

Figure 4. Half-peak time $t_{1/2}$ vs. Q for C_6D_6 (at left) and for CS_2 (at right) solutions. The continuous lines are theoretical results at T = 30 °C, and the dashed line is at T = 70 °C; points indicated as ○, ●, △, and ▲ are derived from the experimental results from samples 1–4, respectively (see Table I and Figure 3).

If such a dependence were to hold rigorously, the double-logarithmic plots of Figure 4 should appear as straight lines; although this is rather well verified over appropriate intervals of Q, especially for the calculated curves, the exponent appears to decrease somewhat with increasing Q. This is shown numerically in Table IIIa, where the average $\mathcal{B}$'s observed for different Q ranges, both theoretically and experimentally, are reported; once again, the agreement appears to be satisfactory.

We have investigated the separate effects on the theoretical figure of $\mathcal{B}$ due to the good-solvent expansion (i.e., $\tilde{\alpha}^2(q)$, see eq 18), to the hydrodynamic interaction (i.e., h_0, eq 20), and to the internal viscosity (i.e., τ_0, eq 21, 22′); indicative results are given in Table IIIb. (Adding the effects of course is not permissible except to a rough approximation.) While the solvent expansion appears to have a minor importance throughout our Q range, the remarkable decrease of the influence of hydrodynamic interaction for $Q > 0.1$ Å^{-1} suggests that we identify a characteristic range of Q, centered at Q^*, such that we have either the free-draining or the impermeable-coil model depending on whether Q is larger or smaller than this range. It is obvious that Q^* should increase with increasing h_0; the following argument shows that we should approximately expect a linear relationship between these two quantities. First, we assume that there is a scale distance $D^* \propto Q^{*-1}$. Second, D^* may be associated with a Fourier coordinate q^* through $q^{*-1}l^2 \propto D^{*2}$; in fact, the q^* mode represents a wave comprising $2\pi/q^*$ chain atoms per wavelength, and D^{*2} may be identified with the mean-square distance between atoms separated by just one wavelength (for long sequences the mean-square distance is approximately proportional to the contour length). Third, looking at eq 20 the crossover must correspond to $h_0 f(q^*) \approx 1$ and, since it is possible to show from (20^i) that $f(q^*) \propto q^{*-1/2}$ (provided $q^* \ll 1$, $q^*N \gg 1$), by substitution we get

$$Q^* \propto h_0/l \tag{34}$$

For $Q > Q^*$ the intramolecular properties should dominate the dynamics for any polymer concentration (even in a melt, entanglement or reptation effects do not appear to be observable for $Q > 0.05$ Å^{-1} [38]). For $Q < Q^*$ and in dilute solution, we should approach $\mathcal{B} = 3$ (Zimm limit), independently of the configurational chain properties.[39] In contrast, it should be pointed out that the $\mathcal{B}$ exponent observable at $Q > Q^*$ may range in principle from 4 for a very flexible chain (Rouse model) to less than 3 for a very rigid chain.[8] It is noticeable that the experimental figure of $\mathcal{B}$ is close to 2 at higher Q (Table IIIa); from our calculations this result is clearly seen as due to intramolecular factors only, namely the configurational rigidity (i.e., the sharp-peaked $C(q)$[8]) and the internal viscosity,[9c] in agreement with previous theoretical analyses. In another study the decrease of $\mathcal{B}$ below 3 at higher Q was already clearly recognized; it was attributed to the approach to the single-bead motion within an appropriate bead-and-spring model.[40] We remark here that the same idea that many degrees of freedom are effectively inactive (frozen) in the localized motions at higher Q is still present in the approach of this paper, in spite of a more elaborate physical picture. The small, not quite significant increase of the experimental $\mathcal{B}$ ($0.05 \leq Q \leq 0.16$ Å^{-1}) upon increasing T from 30 to 70 °C may be due to the temperature dependence of the internal viscosity (see eq 24).

The very small value of R_{eff} derived from ζ (~0.4 Å, see Table II) suggests inadequacy of Stokes' law at the level of the single monomeric units, at least in its current in-

terpretation. Perhaps this result may be qualitatively reconciled with the molecular dynamics investigations of Brey and Gómez Ordóñez who find that, for given densities of the solute and the solvent, the friction constant becomes smaller than expected from Stokes' law when their molecular masses have comparable values.[41] Since our range of observation lengths is relatively small, being of the order of a few tens of angstroms, the normal modes contributing to the time decay of $S(Q,t)$ are relatively localized and consequently the effective polymer mass may not be much larger than that of the solvent. This interpretation seems to be qualitatively consistent with the fact that we get a larger value for R_{eff} (=2.76 Å) from a previous best fit on the frequency axis between the calculated and experimental data of the complex modulus[9c] where the *collective* chain modes tend to give a substantial contribution. Besides, it should be pointed out that the viscosity of the solvents used for the mechanical measurements (i.e., chlorinated diphenyls, $\eta_s \simeq 70$ P[17]) is about 10^4 times larger than that of the present solvents. From our results we may suggest that, with solvents of comparable viscosity and in a reasonably limited range of time and temperature, a suitably parametrized form of Stokes' law works reasonably well, considering that the calculations reported in Figures 3 and 4 are carried out with a single value of R_{eff}.

It should not be forgotten that we have another independent source of the ratio ζ/η_s, namely the parameter $h_0 = 0.03$ (see ref 9c and Table II), whence $R_{eff} = 0.125$ Å. Even considering that the classical Oseen theory in the preaveraged form may not be fully adequate in quantitative terms, it is worth mentioning that Kirkwood and Riseman obtained results in the same range as ours, from zero-frequency measurements on polystyrene solutions where the hydrodynamic interaction appears to be the dominating factor (they get $\zeta/\eta_s = 2.5 \times 10^{-8}$ and 10.5×10^{-8} cm from benzene and butanone solutions,[42] whence the respective R_{eff}'s are 0.12 and 0.57 Å, see eq 23).

Concluding Remarks

A theoretical investigation based on quasi-elastic neutron scattering results from atactic polystyrene solutions in the range $0.05 < Q < 0.3$ Å^{-1} has been carried out. We have taken into account what are currently considered as the most important factors, namely (i) the intramolecular elasticity, (ii) the internal viscosity, (iii) the hydrodynamic interaction, and (iv) the excluded-volume effect. Factor i has been taken care of by extending the calculation of the generalized characteristic ratio $C(q)$ from the simple case of an $-[A]_N-$ polymer[7,8] to that of an $-[A-B]_N-$ chain with a random distribution of stereoisomeric centers; for the range under investigation we have shown that this polymer may be treated as an equivalent $-[A]_{2N}-$ chain with appropriate parameters, thus simplifying the problem. Factors ii–iv have been embodied in the linear dynamic equations via the parameters τ_0, h_0, and $\bar{\beta}$, respectively, which in turn have been estimated from previous experimental measurements.[17-20] The Fourier configurational representation of the chain dynamical modes permits a self-consistent treatment of all the variables, within the whole range of interatomic distances.[7-10] The only parameter to be determined was the effective radius per chain atom R_{eff}, which gives the friction coefficient ζ through Stokes' law (see eq 23), hence the time unit t_0 (eq 16); the interatomic correlation function $B(k,t)$ is then obtainable from eq 22 and consequently the coherent dynamic structure factor $S_{coh}(Q,t)$ from eq 32.

Choosing the best-fitting value of R_{eff}, our results show a satisfactory agreement with experiment. Indicating with $t_{1/2}$ the half-peak time of $S_{coh}(Q,t)$, at sufficiently low values of Q ($\lesssim 0.1$ Å^{-1}) the $\mathcal{B}$ exponent of the power law $t_{1/2}Q^{\mathcal{B}} \simeq$ const is close to 3, according to the theoretical predictions for an impermeable coil. At higher Q's the hydrodynamic effect tends to vanish and the joint influence of the configurational rigidity and of the internal viscosity leads to a further reduction of $\mathcal{B}$ to a value around 2. The excluded-volume effect appears to be small in the whole Q-range.

It should be stressed that within the present theoretical investigation some fast-relaxing motions are deliberately ignored. In fact, in addition to disregarding the small amplitude chain normal modes with the short relaxation times $\tau_2(q)$ (see eq 13), we have assumed that the scattering power is concentrated on the chain atoms, thus implying that the scattering by the nuclei of the phenyl rings is also neglected. However, although the size of these rings ($\approx$3–5 Å) is not negligible compared with the shortest distances probed by the radiation ($\approx 2\pi/Q_{max} \approx 20$ Å), it is realistic to assume that their scattering contribution should relax more quickly than that of the chain, due to their relatively fast motions. In conclusion, the $S(Q,t)$ curves should be characterized by a somewhat faster initial decay than displayed by our calculations (see Figure 3). It is reasonable to expect that the related error should be mainly reflected upon the calculated $t_{1/2}$, much less upon the exponent $\mathcal{B}$.

Work is in progress to extend the present investigation to other polymers showing different degrees of flexibility, with the purpose of comparing specific properties of different polymer chains outside the universal ranges.

Acknowledgment. One of the authors (G.A.) acknowledges very helpful discussions with Dr. S. Stühn (Institut für Physikalische Chemie, Mainz, West Germany). The present work was made possible by a financial contribution from the Progetto Finalizzato per la Chimica Fine e Secondaria, Consiglio Nazionale delle Ricerche, Italy.

Appendix

The x-projection of the elastic force acting on the kth chain atom is, from eq 10 and by using eq 7 and 9

$$f_x(2\mu - 1) = \frac{3k_BT}{4Nl^2}\sum_{|q|}[1 - \exp(iq)]\exp(-i\mu q)\{\tilde{x}_A(q)U(q) - \tilde{x}_B(q)U^*(q)\} \quad \text{(A-1a)}$$

$$f_x(2\mu) = \frac{3k_BT}{4Nl^2}\sum_{|q|}[1 - \exp(iq)]\exp(-i\mu q) \times \{\tilde{x}_A(q)V(q) - \tilde{x}_B(q)V^*(q)\exp(-iq)\} \quad \text{(A-1b)}$$

where

$$U(q) = [\lambda^{-1}(q) - \mu^{-1}(q)]\exp[i\Delta(q)] - [\lambda^{-1}(q) + \mu^{-1}(q)] \quad \text{(A-2a)}$$

$$V(q) = [\lambda^{-1}(q) + \mu^{-1}(q)]\exp(-iq) - [\lambda^{-1}(q) - \mu^{-1}(q)]\exp[i\Delta(q)] \quad \text{(A-2b)}$$

To obtain the Fourier transform of the dynamical equations (11), we must express the coordinates $x(2\mu)$ and $x(2\mu - 1)$ in terms of $\tilde{x}_A(q)$ and $\tilde{x}_B(q)$ ($q \neq 0$). From the relationship (see Figure 1, $x(0) \equiv x(2N)$)

$$x(k) - x(0) = [\sum_{h=1}^{k}\mathbf{l}(h)]_x \quad \text{(A-3)}$$

assuming $x(0) \equiv 0$ and antitransforming eq 6 to get $\mathbf{l}(h)$, we have

$$x(2\mu - 1) = (2N)^{-1}\sum_{\{q\}}{}'\exp(-i\mu q)\{\tilde{x}_A(q) + \tilde{x}_B(q)\exp(iq)\} \quad \text{(A-4a)}$$

$$x(2\mu) = (2N)^{-1}\sum_{\{q\}}{}'\exp(-i\mu q)\{\tilde{x}_A(q) + \tilde{x}_B(q)\} \quad \text{(A-4b)}$$

the prime on the sum symbol meaning that the term with $q = 0$ is excluded.

The Fourier transform of eq 11 is now given as ($q \neq 0$)

$$-\frac{3k_BT}{2l^2}[1 - \exp(iq)]\{\tilde{x}_A(q,t)U(q) - \tilde{x}_B(q,t)U^*(q)\} + \zeta_1\{\dot{\tilde{x}}_A(q,t) + \dot{\tilde{x}}_B(q,t)\exp(iq)\} = 2\tilde{X}_1(q,t) \quad \text{(A-5a)}$$

$$-\frac{3k_BT}{2l^2}[1 - \exp(iq)]\{\tilde{x}_A(q,t)V(q) - \tilde{x}_B(q,t)V(q)\exp(-iq)\} + \zeta_2\{\dot{\tilde{x}}_A(q,t) + \dot{\tilde{x}}_B(q,t)\} = 2\tilde{X}_2(q,t) \quad \text{(A-5b)}$$

where

$$\tilde{X}_{1(2)}(q,t) = \sum_{\mu=1}^{N}\exp(i\mu q)X_{1(2)}(\mu,t) \quad \text{(A-6)}$$

The average properties of $\tilde{X}_h$ ($h = 1, 2$) are specified by the fluctuation-dissipation theorem[43]

$$\langle\tilde{X}_h(q,t)\tilde{X}_k(q',t')\rangle = 2Nk_BT\zeta_h\Delta(h - k)\Delta(q + q')\delta(t - t') \quad \text{(A-7)}$$

where $h, k = 1, 2$, while Δ and δ respectively are the Kronecker delta and the Dirac delta function. Omitting for brevity the arguments q and t, eq A-5 may be written

$$a_1\dot{\tilde{x}}_A + b_1\dot{\tilde{x}}_B + c_1\tilde{x}_A + d_1\tilde{x}_B = 2\tilde{X}_1 \quad \text{(A-8a)}$$

$$a_2\dot{\tilde{x}}_A + b_2\dot{\tilde{x}}_B + c_2\tilde{x}_A + d_2\tilde{x}_B = 2\tilde{X}_2 \quad \text{(A-8b)}$$

The solution of this system is reported in eq 12 in terms of the unknown functions $\rho_{1(2)}(q,t)$ and $\sigma_{1(2)}(q,t)$ and $\tau_{1(2)}(q)$. In order to obtain these functions, we substitute eq 12 in eq A-8 and have (dropping the q variable for simplicity)

$$\int_{-\infty}^{t}\left\{[-a_1\rho_1(t')/\tau_1 - b_1\sigma_1(t')/\tau_1 + c_1\rho_1(t') + d_1\sigma_1(t')]\exp\left(-\frac{t - t'}{\tau_1}\right) + [-a_1\rho_2(t')/\tau_2 - b_1\sigma_2(t')/\tau_2 + c_1\rho_2(t') + d_1\sigma_2(t')]\exp\left(-\frac{t - t'}{\tau_2}\right)\right\}dt' + a_1[\rho_1(t) + \rho_2(t)] + b_1[\sigma_1(t) + \sigma_2(t)] = 2\tilde{X}_1(t) \quad \text{(A-9a)}$$

$$\int_{-\infty}^{t}\left\{[-a_2\rho_1(t')/\tau_1 - b_2\sigma_1(t')/\tau_1 + c_2\rho_1(t') + d_2\sigma_1(t')]\exp\left(-\frac{t - t'}{\tau_1}\right) + [-a_2\rho_2(t')/\tau_2 - b_2\sigma_2(t')/\tau_2 + c_2\rho_2(t') + d_2\sigma_2(t')]\exp\left(-\frac{t - t'}{\tau_2}\right)\right\}dt' + a_2[\rho_1(t) + \rho_2(t)] + b_2[\sigma_1(t) + \sigma_2(t)] = 2\tilde{X}_2(t) \quad \text{(A-9b)}$$

In view of the stochastic nature of $\tilde{X}_1(t)$ and $\tilde{X}_2(t)$ the functions within the integrals must identically vanish, and thus the following secular equation is obtained

$$\mathrm{Det}\begin{bmatrix} c_1 - a_1/\tau & d_1 - b_1/\tau \\ c_2 - a_2/\tau & d_2 - b_2/\tau \end{bmatrix} = 0 \quad \text{(A-10)}$$

τ being either τ_1 or τ_2. This gives for τ_1 and τ_2, after substituting the symbols $(a_h \cdots d_h)$ from eq A-2 and A-5

$$\tau_1(q) = \frac{l^2\{W(q) + \sqrt{W^2(q) - 8\zeta_1\zeta_2\lambda(q)\mu(q)(1 - \cos q)}\}}{12k_BT(1 - \cos q)} \quad \text{(A-11a)}$$

$$\tau_2(q) = \frac{l^2\{W(q) - \sqrt{W^2(q) - 8\zeta_1\zeta_2\lambda(q)\mu(q)(1 - \cos q)}\}}{12k_BT(1 - \cos q)} \quad \text{(A-11b)}$$

where

$$W(q) = (\zeta_1 + \zeta_2)[\lambda(q) + \mu(q)] + [\zeta_1\cos(q + \Delta(q)) + \zeta_2\cos\Delta(q)][\lambda(q) - \mu(q)] \quad \text{(A-12)}$$

Equating to zero the four coefficients of the time exponentials in (A-9) gives two independent equations. A further two are obtained from the residual parts of the equations outside the time integrals; solving these four equations gives expressions for ρ_1, ρ_2, σ_1, and σ_2 as follows:

$$\rho_1 = K\tau_2[\tilde{X}_1(d_2\tau_1 - b_2) + \tilde{X}_2(b_1 - d_1\tau_1)] \quad \text{(A-13a)}$$

$$\rho_2 = K\tau_1[\tilde{X}_1(b_2 - d_2\tau_2) + \tilde{X}_2(d_1\tau_2 - b_1)] \quad \text{(A-13b)}$$

$$\sigma_1 = K\tau_2[\tilde{X}_1(a_2 - c_2\tau_1) + \tilde{X}_2(c_1\tau_1 - a_1)] \quad \text{(A-13c)}$$

$$\sigma_2 = K\tau_1[\tilde{X}_1(c_2\tau_2 - a_2) + \tilde{X}_2(a_1 - c_1\tau_2)] \quad \text{(A-13d)}$$

and

$$K = \frac{2}{(\tau_1 - \tau_2)(a_1b_2 - a_2b_1)} \quad \text{(A-14)}$$

Registry No. Polystyrene (homopolymer), 9003-53-6; neutron, 12586-31-1.

References and Notes

(1) P.-G. de Gennes, "Scaling Concepts in Polymer Physics", Cornell University Press, Ithaca, 1979, Chapter 5.
(2) G. Allen, R. Ghosh, J. S. Higgins, J. P. Cotton, B. Farnoux, G. Jannink, and G. Weill, *Chem. Phys. Lett.*, **38**, 577 (1976).
(3) J. S. Higgins, G. Allen, R. E. Ghosh, W. S. Howells, and B. Farnoux, *Chem. Phys. Lett.*, **49**, 197 (1977).
(4) L. K. Nicholson, J. S. Higgins, and J. B. Hayter, *Macromolecules*, **14**, 836 (1981).
(5) J. S. Higgins, L. K. Nicholson, and J. B. Hayter, *Polymer*, **22**, 163 (1981).
(6) G. Ronca, *J. Chem. Phys.*, **67**, 4965 (1977).
(7) G. Allegra, *J. Chem. Phys.*, **68**, 3600 (1978).
(8) G. Allegra and F. Ganazzoli, *J. Chem. Phys.*, **74**, 1310 (1981).
(9) (a) G. Allegra, *J. Chem. Phys.*, **61**, 4910 (1974). (b) G. Allegra, *ibid.*, **63**, 599 (1975). (c) G. Allegra and F. Ganazzoli, *Macromolecules*, **14**, 1110 (1981).
(10) G. Allegra and F. Ganazzoli, *J. Chem. Phys.*, **76**, 6354 (1982).
(11) W. Kuhn, *Kolloid-Z.*, **76**, 258 (1936); **87**, 3 (1939).
(12) P. E. Rouse, *J. Chem. Phys.*, **21**, 1272 (1953).
(13) B. H. Zimm, *J. Chem. Phys.*, **24**, 269 (1956).
(14) H. A. Kramers, *Physica*, **7**, 284 (1940).
(15) S. F. Edwards and K. F. Freed, *J. Chem. Phys.*, **61**, 1189 (1974).
(16) G. Ronca, private communication, 1977.
(17) D. J. Massa, J. L. Schrag, and J. D. Ferry, *Macromolecules*, **4**, 210 (1971).
(18) K. Osaki and J. L. Schrag, *Polym. J.*, **2**, 541 (1971).
(19) K. Osaki, *Adv. Polym. Sci.*, **12**, 1 (1973).
(20) B. Nyström and J. Roots, *Prog. Polym. Sci.*, **8**, 333 (1982).
(21) See, e.g., C. Kittel, "Introduction to Solid State Physics", J. Wiley and Sons, New York, 1971.
(22) G. Allegra and F. Ganazzoli, *Macromolecules*, **16**, 1311 (1983).
(23) P. J. Flory, *J. Chem. Phys.*, **17**, 303 (1949).
(24) G. Allegra, *Macromolecules*, **16**, 555 (1983).
(25) G. Allegra and F. Ganazzoli, *Macromolecules*, **16**, 1392 (1983).
(26) D. Y. Yoon, P. R. Sundararajan, and P. J. Flory, *Macromolecules*, **8**, 776 (1975).
(27) E. Helfand, *J. Chem. Phys.*, **54**, 4651 (1971).
(28) M. Fixman, *J. Chem. Phys.*, **69**, 1538 (1978).
(29) G. Allegra and S. Brückner, *Macromolecules*, **10**, 106 (1977).
(30) U. W. Suter and P. J. Flory, *Macromolecules*, **8**, 765 (1975).
(31) Information from the Scientific Secretary, Institut Laue-Langevin, 38042 Grenoble, France.
(32) F. Mezei, Ed., *Lect. Notes Phys.*, **128**, (1980).

(33) The resolution of about 10^{-7} s^{-1} restricted the reliability of data for these samples to values of $Q > 0.03$ Å^{-1}. On the other hand, the coherent signal intensity became too low for reliable analyses for values of $Q > 0.15$ Å^{-1}.
(34) M. Birr, A. Heidemann, and B. Alefeld, *Nucl. Instrum. Methods*, **95**, 435 (1971).
(35) W. S. Howells, Rutherford and Appleton Laboratory report RL-81-039.
(36) B. J. Berne and R. Pecora, "Dynamic Light Scattering with Applications to Chemistry, Biology and Physics", Wiley-Interscience, New York, 1976.
(37) A closed expression of $S(Q,t)$ was previously obtained for ring polymers with freely jointed links and $N \to \infty$ by A. Z. Akcasu, M. Benmouna, and C. C. Han, *Polymer*, **21**, 866 (1980).
(38) D. Richter, A. Baumgärtner, K. Binder, B. Ewen, J. B. Hayter, *Phys. Rev. Lett.*, **47**, 109 (1981).
(39) M. Benmouna and A. Z. Akcasu, *Macromolecules*, **11**, 1187 (1978).
(40) A. Z. Akcasu and J. S. Higgins, *J. Polym. Sci., Polym. Phys. Ed.*, **15**, 1745 (1977).
(41) J. J. Brey and J. Gómez Ordóñez, *J. Chem. Phys.*, **76**, 3260 (1982).
(42) J. G. Kirkwood and J. Riseman, *J. Chem. Phys.*, **16**, 565 (1948).
(43) H. Mori, *Prog. Theor. Phys.*, **33**, 423 (1965).

Excluded Volume Effects in the Θ Regime. 1. Perturbation Formulation for a Repulsive–Attractive Potential†

James E. Martin

Division 1152, Sandia National Laboratories, Albuquerque, New Mexico 87185.
Received June 20, 1983

ABSTRACT: Perturbation methods are used to develop a theory of dilute polymer solutions in the Θ regime. The theory assumes that a polymer can be represented as a Gaussian random walk that interacts through a pairwise potential. The formulation is graph theoretical and is developed in a way that is independent of polymer topology. Various properties are treated: scattering and pair correlation functions, the end-to-end vector, the radius of gyration, the hydrodynamic radius, and the second virial coefficient. Unlike δ-function theory, the excluded volume potential used here is bounded and contains repulsive and attractive interactions. These interactions persist at the Θ temperature and give a reference state that is non-Gaussian, except in the δ-function limit of the theory. Several conclusions are reached: (1) the Θ chain is swollen relative to the unperturbed chain (no interactions) but this swelling does not affect the ratio of the radius of gyration to the end-to-end vector; (2) the swelling is greater for the hydrodynamic radius than the radius of gyration (non-Gaussian behavior); (3) a universal excluded volume parameter (hence a two-parameter theory) is found only in the δ-function limit. Finally, it is shown that in the short-range interaction limit the theory can be generalized to arbitrary excluded volume potentials by introducing a dimensionless parameter that is related to the second moment of the cluster formation.

I. Introduction

The δ-function perturbation theory of the excluded volume effect, due to Fixman,[1] has come under close scrutiny in recent years. Most of the recent interest has centered on the convergence properties of the cluster series and on the assumption that two-body interactions provide an adequate description of the Θ regime. In this connection it has been suggested by Edwards[2] and Gordon et al.[3] that the perturbation series for expansion factors is actually divergent (this does not necessarily limit its utility for calculations, however, since the series appears to be asymptotic). Aronowitz and Eichinger[4] have explicitly demonstrated the presence of divergences in the series for expansion factors of small chains. They trace this difficulty to the δ-function potential (a preaveraged cluster function) and estimate a radius of convergence of order $1/N^{1/2}$ for the cluster series. Oono[5] has demonstrated that the perturbation series is an expansion about a singular point (a collapse transition for infinite chains) and has also estimated a radius of convergence of order $1/N^{1/2}$.

Oyama and Oono[6] have expressed doubt that the many-body interactions in a real polymer chain can be expressed in terms of the segment binary cluster integral alone—a measure of binary contacts. They include the effect of three-body interactions and find that these tend to swell the polymer at the Θ point (a specific solvent effect), without affecting exponents.

Monte Carlo simulations of lattice and continuum chains have been done for poor, marginal, and good solvents. These studies represent a polymer chain as an interacting walk whose many-body potential can be approximated by a sum of pairwise interactions between segments. The potential has a temperature-dependent parameter that can be adjusted to achieve the desired solvent condition. Excluded volume potentials chosen for such studies differ in two ways from the δ potential: they are of nonvanishing width and do not identically vanish at the Θ temperature. In these studies the Θ condition is achieved by balancing the repulsive core interaction against an attractive interaction that occurs at larger distances. We will refer to this chain as the Θ chain so as to distinguish it from the unperturbed chain (no excluded volume interactions).

Baumgartner[7] and Webman et al.[8] have simulated continuum chains with Lennard-Jones interactions. Baumgartner has found that at the Θ point, defined by the vanishing of the second virial coefficient, the exponent for the polymer radius is $^1/_2$ but the chain is swollen relative to the unperturbed state. In fact, for the width of the excluded volume potential chosen by Baumgartner, $\langle R^2\rangle_\Theta/\langle R^2\rangle_0 \sim 1.7$, where the subscripts refer to the Θ and unperturbed chain, respectively.

It would seem that this swelling is not of any real significance in itself, since an appropriately renormalized unperturbed chain would be equivalent to the Θ chain insofar as the radius of gyration is concerned. It is not clear, however, that this renormalized chain is equivalent to the Θ chain in all its properties. For example, obvious differences between these models would arise in the calculation of exponents for the radius in 1 and 2 dimensions.

†This work performed at Sandia National Laboratories supported by the U.S. Department of Energy under Contract No. DE-AC04-76DP00789.

0024-9297/84/2217-1263$01.50/0